Journal of Instrumentation

Test and characterization of 400 Hamamatsu R5912-MOD photomultiplier tubes for the ICARUS T600 detector

To cite this article: M. Babicz *et al* 2018 *JINST* **13** P10030

Published by IOP Publishing for Sissa Medialab

Received: *August 27, 2018*
Accepted: *October 16, 2018*
Published: *October 26, 2018*

Test and characterization of 400 Hamamatsu R5912-MOD photomultiplier tubes for the ICARUS T600 detector

The ICARUS/NP01 Collaboration

M. Babicz,[a,b] **L. Bagby,**[c] **B. Baibussinov,**[d] **V. Bellini,**[e] **M. Bonesini,**[f] **A. Braggiotti,**[d,g] **S. Centro,**[d] **T. Cervi,**[h] **A.G. Cocco,**[i] **A. Falcone,**[h,j] **C. Farnese,**[d] **A. Fava,**[c,d] **F. Fichera,**[e] **D. Gibin,**[d] **A. Guglielmi,**[d] **U. Kose,**[b] **R. Mazza,**[f] **A. Menegolli,**[h] **G. Meng,**[d] **C. Montanari,**[h] **M. Nessi,**[b] **P. Picchi,**[h] **F. Pietropaolo,**[b,d] **M.C. Prata,**[h] **A. Rappoldi,**[h] **G.L. Raselli,**[h,1] **M. Rossella,**[h] **C. Rubbia,**[b,k,l,2] **P. Sala,**[b] **A. Scaramelli,**[h] **F. Sergiampietri,**[m] **M. Spanu,**[h,3] **M. Torti,**[f] **F. Tortorici,**[e] **F. Varanini,**[d] **S. Ventura,**[d] **C. Vignoli**[l] **and A. Zani**[b]

[a] *Institute of Nuclear Physics PAN, Cracow, Poland*
[b] *CERN, Geneva, Switzerland*
[c] *Fermi National Laboratory, Batavia IL, U.S.A.*
[d] *University of Padova and INFN, Padova, Italy*
[e] *University of Catania and INFN, Catania, Italy*
[f] *University of Milano Bicocca and INFN, Milan, Italy*
[g] *CNR, Padova, Italy*
[h] *University of Pavia and INFN, Pavia, Italy*
[i] *University of Napoli and INFN, Napoli, Italy*
[j] *University of Texas in Arlington, Arlington TX, U.S.A.*
[k] *Gran Sasso Science Institute, L'Aquila, Italy*
[l] *INFN, Laboratori Nazionali del Gran Sasso, Assergi, Italy*
[m] *INFN, Pisa, Italy*

E-mail: gianluca.raselli@pv.infn.it

Abstract: ICARUS T600 will be operated as far detector of the Short Baseline Neutrino program at Fermilab (U.S.A.), which foresees three liquid argon time projection chambers along the Booster Neutrino Beam line to search for a LSND-like sterile neutrino signal. The detector employs 360 photomultiplier tubes, Hamamatsu model R5912-MOD, suitable for cryogenic applications. A total of 400 PMTs were procured from Hamamatsu and tested at room temperature to evaluate the performance of the devices and their compliance to detect the liquid argon scintillation light in the T600 detector. Furthermore 60 units were also characterized at cryogenic temperature, in liquid

[1] Corresponding author.
[2] Spokesman.
[3] Now at Brookhaven National Laboratory, NY, U.S.A.

https://doi.org/10.1088/1748-0221/13/10/P10030

2018 JINST 13 P10030

argon bath, to evaluate any parameter variation which could affect the scintillation light detection. All the tested PMTs were found to comply with the requirements of ICARUS T600 and a subset of 360 specimens was selected for the final installation in the detector.

KEYWORDS: Photon detectors for UV, visible and IR photons (vacuum) (photomultipliers, HPDs, others); Noble liquid detectors (scintillation, ionization, double-phase); Time projection chambers

ARXIV EPRINT: 1807.08577

2018 JINST 13 P10030

Contents

2018 JINST 13 P10030

1 Introduction

ICARUS T600 detector is the largest Liquid Argon Time Projection Chamber (LAr-TPC) ever built for neutrino oscillation studies, successfully operated at LNGS (Laboratori Nazionali del Gran Sasso) underground laboratory (Italy) [1]. It took data from 2010 to 2013 exposed to the CNGS (CERN Neutrinos to Gran Sasso) beam from CERN and atmospheric neutrinos with a live-time factor in excess of 93% [2]. After an intense refurbishing operation, carried out at CERN in the framework of the Neutrino Platform (NP01) activities, the entire apparatus was transferred to Fermilab (IL, U.S.A.). It will become the far detector of the Short Baseline Neutrino (SBN) program [3], exploiting three liquid argon detectors, placed along the Booster Neutrino Beam (BNB) line and operating at shallow depth, to investigate the possible presence of sterile neutrino states.

The realization of a new liquid argon scintillation light detection system, with high performance photomultiplier tubes (PMTs) represents a primary task of the detector refurbishing. Since the detector will be subject to a huge cosmic flux, the light detection system would allow the 3D reconstruction of events contributing to the identification of neutrino interactions in the beam spill gate.

The T600 scintillation light detection system was significantly upgraded at CERN from summer 2015 to summer 2017. The 74 outdated ETL 9357FLA PMTs mounted in the detector in 2000 [1, 4] were replaced with new 360 Hamamatsu R5912-MOD units operating in liquid argon. Each PMT was tested and characterized to determine its basic functionality and to verify its compliance with the required functioning specifications. In particular all the PMTs were tested at room temperature

and 60 units were also characterized at cryogenic temperature, in liquid argon bath. Measurements were carried out in different areas at CERN, where a dedicated dark-room and a cryogenic test facility were set-up.

This paper describes this test campaign. In particular, in section 2 the ICARUS T600 scintillation light detection system is described. The main features of the R5912-MOD are presented in section 3. Section 4 describes the employed measurement equipment and the CERN test facilities. Results are reported in section 5. A description of the base layout is also presented in appendix A.

2 The ICARUS T600 scintillation light detection system

ICARUS T600 detector is made of two identical cryostats, each housing two TPCs with a common central cathode. Charged particles interacting in liquid argon produce both scintillation light and ionization electrons. These latter are drifted by a uniform electric field ($E = 500$ V/cm) to the anode, made of three parallel wire planes at 1.5 m from the cathode, where they are collected. Photons are detected by a PMT system with the devices mounted behind the wire planes and operating immersed in liquid argon ($T = 87$ K). The information coming from both scintillation light and collected electrons allows obtaining a full 3D reconstruction of the interacting particle path.

The upgraded T600 light detection system consists of 360 Hamamatsu R5912-MOD PMTs deployed behind the 4 TPC wire chambers, 90 units each. Before installation the sensitive window of each PMT was coated with about 200 μg/cm^2 of Tetra-Phenyl Butadiene (TPB), a wavelength shifter to convert VUV LAr scintillation photons ($\lambda = 128$ nm) to visible light. This process was performed using a dedicated thermal evaporator and a specific deposition technique [5, 6]. Mechanical supports were designed to hold up each PMT in the proper position at few millimeters behind the TPC wire planes. Each device is set inside a grounded stainless-steel cage to prevent the induction of PMT pulses on the facing wire plane. Furthermore a 50 µm optical fiber directed towards the sensitive surface will allow a timing calibration at nanosecond precision. A picture of the new light detection system is shown in figure 1.

Figure 1. PMT deployment behind a TPC wire plane.

2018 JINST 13 P10030

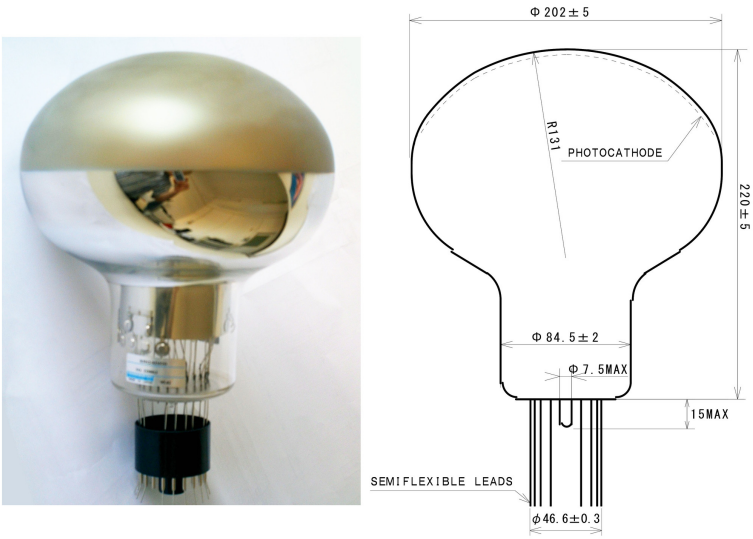

Figure 2. The PMT Hamamatsu R5912-MOD. Lengths are in millimeters in the right figure [7]. Reproduced from [7] with permission.

3 The Hamamatsu R5912-MOD

The Hamamatsu R5912-MOD is a 10-dynode-stage PMT with an 8 in hemispherical photocathode (see figure 2). The PMT is derived from the parent model R5912. The bialkali photocathode is deposited on a Pt under-layer in order to extend the range of the operating temperature down to about −200°C. This PMT model was selected as a result of experimental tests carried out on different detectors samples provided by different producers, such as Hamamatsu and ETL. The main features of the Hamamatsu R5912-MOD resulting from these tests can be summarized as follows [8–10]:

- Nominal PMT gain ($G \approx 10^7$) and quantum efficiency ($\approx$ 15%) which are suitable for the detection of scintillation light produced by ionizing particle with energy $\leq$ 100 MeV;
- Good uniformity of the cathodic sensitivity all over the whole PMT window surface (±10%);
- Good performances in terms of electron transit time spread ($\sigma \approx 1$ ns) and electron transit time variation over the whole PMT window surface, both at room and in cryogenic environment;
- Linear anodic response as a function of the incident light intensity, both at room temperature and in cryogenic environment;
- Pulse gain saturation above 300 photoelectrons.

A pre-series of 20 samples was delivered by Hamamatsu in 2015 for compliance testing purposes and 380 units in 2016. PMTs were selected by the producer to fulfill the performance of table 1 at room temperature, only. All the PMTs were immersed in liquid nitrogen in factory to certify their mechanical strength at cryogenic temperature.

Each device was provided with a proper base electronic circuit designed according to the voltage distribution ratio recommended by Hamamatsu. This supplies the high voltage for the grids, dynodes and anode, and allows the signal to be picked up directly from the anode. Design

2018 JINST 13 P10030

Table 1. Main acceptance requirements for the Hamamatsu R5912-MOD.

Spectral Response	$300 \div 650$ nm
Window Material	Borosilicate glass (sand blasted)
Photocathode	Bialkali with Pt under-layer
Max supply voltage (anode-cathode)	2000 V
Photocathode Q.E. at 420 nm	$\geq 16\%$
Typical Gain	1×10^7 at 1500 V
Nominal anode pulse rise time*	≤ 4 ns
Nominal P/V ratio*	2.5
Max. dark count rate*	5000 s^{-1}
Max. transit time variation	2.5 ns (center-border)

* Values for $G = 1 \times 10^7$

Figure 3. CERN test facilities for room (left) and cryogenic temperature (right) measurement.

and specifications are presented in appendix A. Bases were directly welded on the PMT flying leads. Since a negative power supply is adopted, two independent coaxial cables are used to provide the PMT with the high voltage and to read out the anode signal.

4 Measuring equipment

All the 400 samples were tested at room temperature and 60 of them were also qualified at cryogenic temperature, in liquid argon bath. Characterization processes and measurement methods were all discussed and agreed with the producer.

A dark-room was arranged at CERN to test in parallel up to 16 PMTs (figure 3 left). In a contiguous electronic workshop, a laser diode was set-up to produce fast light pulses at 405 nm and about 1 kHz repetition rate. The light intensity was set through calibrated optical filters mounted on two-wheel supports, allowing different attenuation combinations ($1 \div 1000$). The light was focused on the PMT windows by means of 100 µm multi-mode optical fibers. A picture of the instrumentation is shown in figure 4.

The characterization at room temperature was carried out using the electronics set-up shown in figure 5. The PMT output was integrated by means of a CANBERRA 2005 charge preamplifier and shaped by means of an ORTEC 570 amplifier. The output distribution was recorded by means

2018 JINST 13 P10030

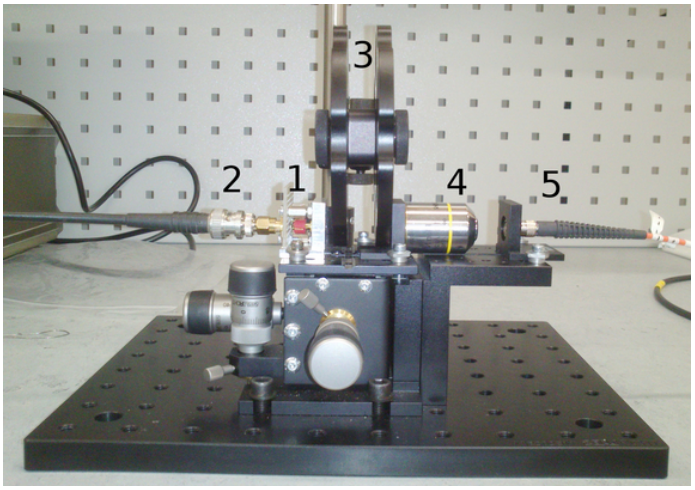

Figure 4. Picture of the adopted laser instrumentation: 1) laser diode; 2 cable from the pulser; 3) rotating filter supports; 4) focusing lens; 5) optical fiber towards the PMT under test.

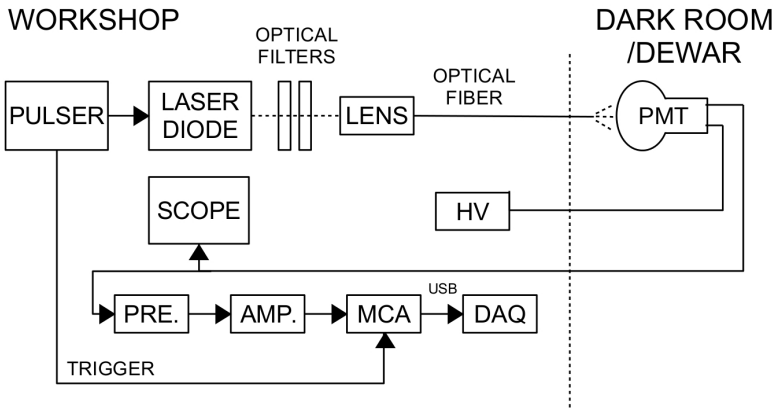

Figure 5. Electronic set-up.

of a 8-k multichannel analyzer CAEN N915. Besides, PMT pulse shapes were acquired by means of a 10 GS/s oscilloscope (LeCroyWaveRunner 104MXI).

Tests at cryogenic temperature were carried out in the building 182 at CERN. In order to obtain experimental conditions similar to those in the real apparatus, PMTs were directly immersed in liquid argon (T = 87 K) inside a large dewar, allowing the simultaneous bath of 10 PMTs (figure 3 right). The internal illumination was achieved by means of a single 100 µm multi-mode optical fiber. The same set-up and acquisition system described above was used together with a proper feed-through, to preserve darkness conditions and thermal insulation.

5 Tests and measurements

Measurements at room temperature were carried out to evaluate the performance of the devices and their conformity to the requested features. Measurements were repeated on a sample of 60 PMTs at

2018 JINST 13 P10030

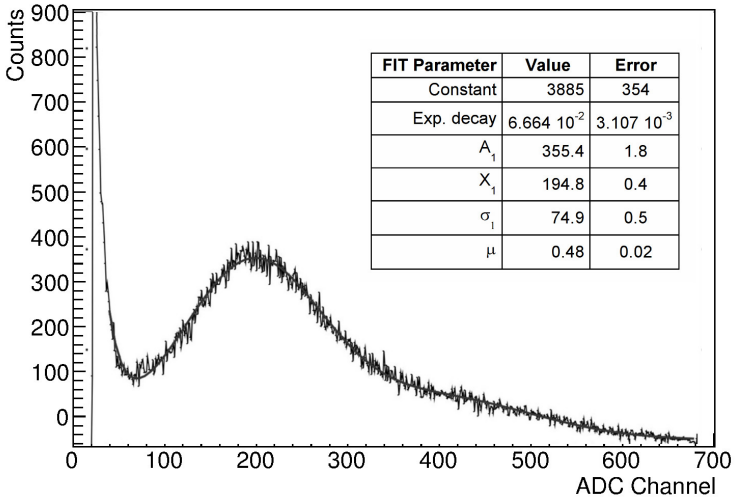

Figure 6. Example of charge distribution for anode signals under single-photon illumination (SER). The result of the fit, using the analytical expression described in the text, is also shown.

cryogenic temperature to evaluate any parameter variation which could affect the scintillation light detection.

5.1 Signal shape

The shapes of the PMT anode pulses were recorded by means of a 10 GHz bandwidth oscilloscope. The PMT illumination was set in order to have single photoelectrons emitted from the cathode, while the resulting anode pulses where directly sampled by the oscilloscope (50 Ω input impedance). Each PMT under test was operated at different temperatures and at a multiplier gain $G \approx 10^7$. No significant variations were observed among the different tested samples and the same mean values resulted at room and at cryogenic temperature: a leading edge of 3.9 ± 1.1 ns, a FWHM of 5.6 ± 1.1 ns and a trailing edge of 10.3 ± 1.6 ns, in good agreement with the nominal values indicated by the manufacturer.

5.2 Single electron response and gain

The response of a PMT to single photoelectrons (SER), i.e., the charge distribution of the PMT pulses integrated over the whole signal shape, is directly related to PMT gain processes. SER studies were carried out by measuring the charge distribution of the PMT pulses induced by single-electron excitation at different power supply values. An example of charge distribution is shown in figure 6.

Charge distributions are characterized by peak profiles which feature a good charge resolution. Spectra were fitted by means of an analytical expression which consists of an exponential distribution, which takes into account PMT and electronic noise, and 3 Gaussian functions which consider the response of the PMT to different photoelectrons. The following parameter constraints were used:

$$X_n = nX_1 \quad \sigma_n = \sigma_1\sqrt{n} \quad A_n = \frac{\mu}{n}A_{n-1}$$

2018 JINST 13 P10030

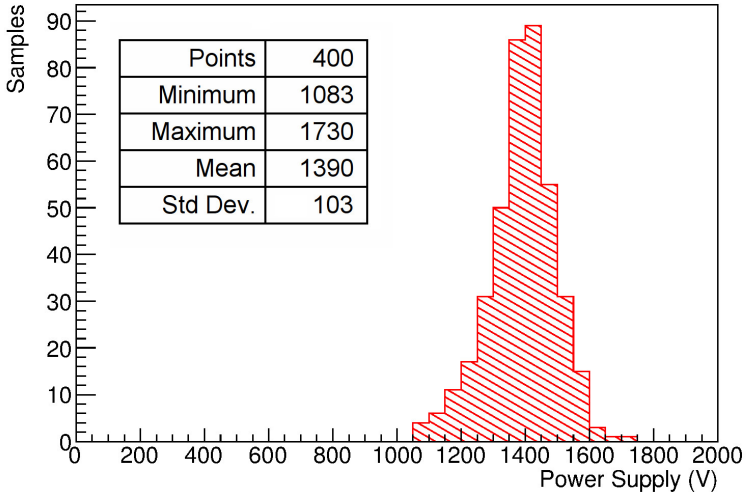

Figure 7. Distribution of voltages to attain a nominal gain $G = 10^7$ for the whole set of 400 PMTs operating at room temperature.

where X_n is the position of the n^{th} Gaussian curve with σ_n width and A_n amplitude. The value of the μ parameter, resulting from the fit, represents the mean of the Poisson distribution of detected photoelectrons.

The position X_1 of the first peak allows the evaluation of the gain G. The gain dependence on the power supply applied to the PMT was measured by changing the voltage setting in a range of values producing PMT gains from about $G = 10^6$ to about $G = 5 \times 10^7$. The PMT nominal voltage was defined as the power supply value to attain a gain $G = 10^7$. The nominal voltage distribution for the whole set of 400 units operating at room temperature is shown in figure 7. The distribution is characterized by a quite narrow spread with mean value set at 1390 V and $\sigma \approx 100$ V.

As an example, the results obtained at room and at cryogenic temperatures, using a single PMT, are plotted in figure 8. The signal amplitude is well represented by a power law behavior as a function of the power supply voltage for both temperatures. A remarkable reduction of the gain is evident at cryogenic temperature with respect to results of measurements at room temperature.

The distribution of the relative gain variation between room and cryogenic temperature, for the whole set of 60 devices tested in both conditions, is plotted in figure 9. Almost all the tested PMTs suffered a gain reduction lasting three days in LAr bath. In this condition, starting from a gain $G = 10^7$, the PMTs showed wide gain decreases down to 10% of nominal values. During the time of observation, the gain values at cryogenic temperature exhibited sudden drops before reaching a stable behavior, affecting the range of variation. Anyway, an increase of less than 150 V of the power supply voltage was on average enough to recover the original gain factors, as shown in figure 10.

The resolution of the SER peak, or relative variance to the peak, defined as the ratio $\sqrt{s} = \sigma_1/X_1$, where X_1 is the SER peak position and σ_1 is the width resulting from the fit, was determined for each PMT. The mean results obtained with the PMTs under test operating at a multiplier gain $G = 10^7$ are:

T = 300 K $\quad \sqrt{s} = 0.35 \pm 0.03$ (Std. Deviation)

T = 87 K $\quad \sqrt{s} = 0.46 \pm 0.11$ (Std. Deviation)

2018 JINST 13 P10030

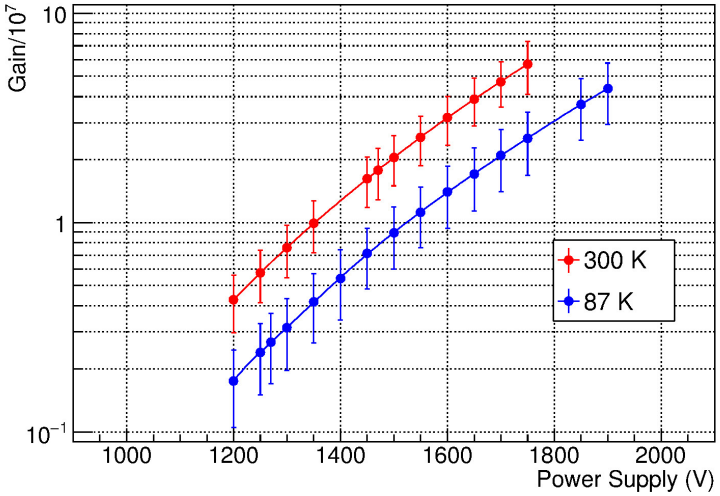

Figure 8. Example of signal amplitude (Gain) as a function of the power supply voltage at room and at cryogenic temperatures for a single PMT. For each measurement the peak position (dots) and the SER distribution width (vertical bars) coming from the fit are shown.

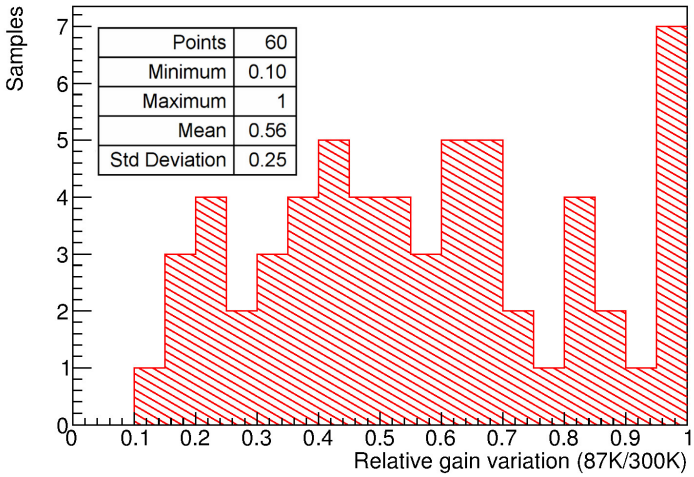

Figure 9. Relative gain variation between room and cryogenic temperatures of the 60 tested PMTs. Results are referred to a power supply consistent with a gain $G = 10^7$ at room temperature.

These values demonstrate the good performance in term of SER charge resolution at both temperature environments, with a slight worsening at 87 K.

5.3 Dark counts and noise

The response of a PMT in absence of light is represented by dark pulses and noise mainly due to ohmic leakage between electrodes on the glass and insulating surfaces of the tubes, thermo-ionic emission of single electrons from the cathode, field emission of electrons induced by local high electric fields inside the PMT.

2018 JINST 13 P10030

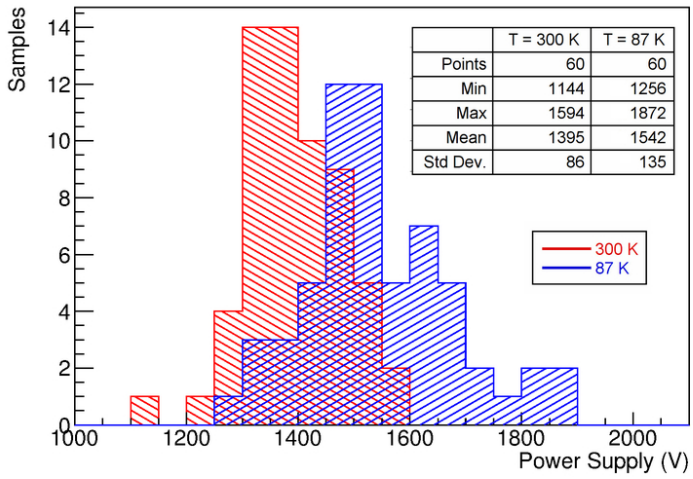

Figure 10. Distribution of voltages to attain a gain $G = 10^7$ both for room and cryogenic temperatures

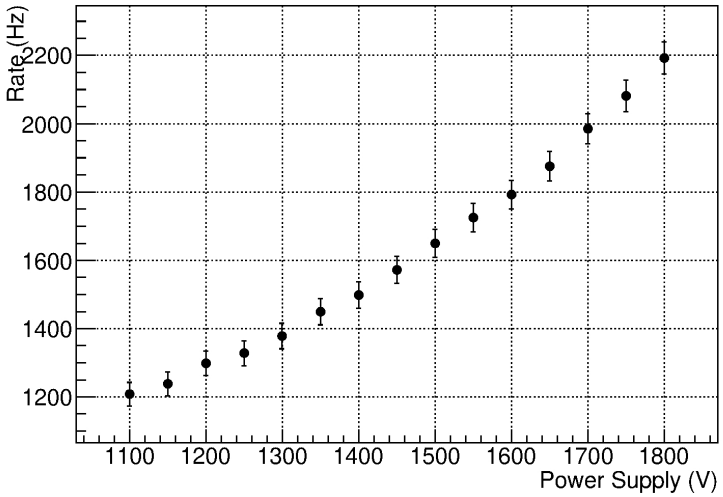

Figure 11. Example of PMT dark rate as a function of the power supplier voltage level. The observed counting spreads are represented with vertical bars.

The dark count rate was evaluated by measuring the rate of the PMT pulses, operating in darkness condition, with the discrimination threshold level set to the minimum value between the pedestal and the maximum of the SER spectrum. An example of dark count rate as a function of the power supply voltage is shown in figure 11, while the distribution obtained at room temperature and at a gain $G = 10^7$ for the 400 tested PMTs is shown in figure 12.

The increase of dark rate when operating a PMT at cryogenic temperature is a well-known effect, referred as Non-Thermal Dark Rate. It was observed and described by many authors, as reported in [11] and in references therein. The precise evaluation of the dark count rate with a PMT directly immersed in liquid argon is not an easy task, due to the presence of Cherenkov radiation

2018 JINST 13 P10030

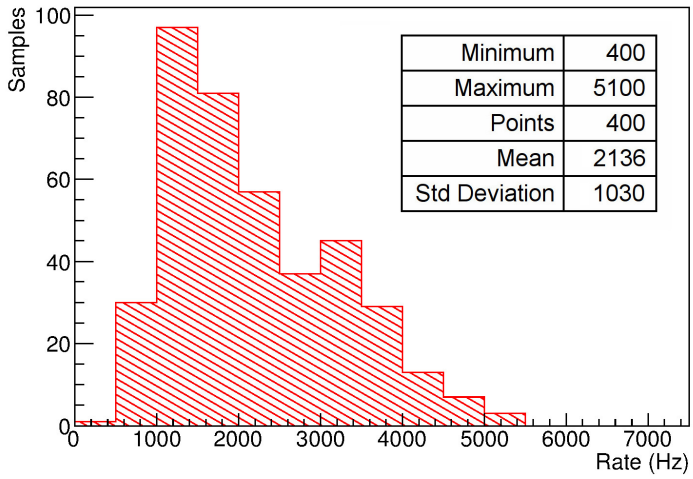

Figure 12. Dark count rate at room temperature for the 400 tested PMTs.

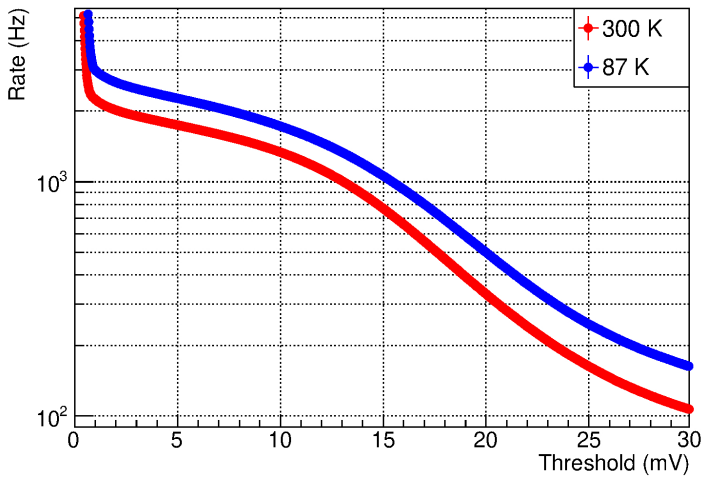

Figure 13. PMT dark count rate as a function of the discrimination threshold at room and at cryogenic temperatures.

and scintillation produced by residual radioactive contaminants, such as ^{39}Ar. In order to prevent these effects, the measurements were carried out using a stainless steel chamber designed to house the PMT under test in vacuum and dark environment. The chamber was placed in a dewar that was filled with liquid argon during the cryogenic measurement. This test, which takes a quite long time for the thermalization, was carried out only on 5 PMT samples. An example of resulting rates, as a function of the discrimination threshold and for the two different operating temperatures is shown in figure 13. The curves were acquired at a multiplier gain $G \approx 10^7$. The spectrum profile is characterized by a hump centered in the region around one photoelectron, caused mainly by the cathode dark noise. An increase of the counting rate at cryogenic temperature, up to a factor 2, was experienced for all the tested PMTs.

2018 JINST 13 P10030

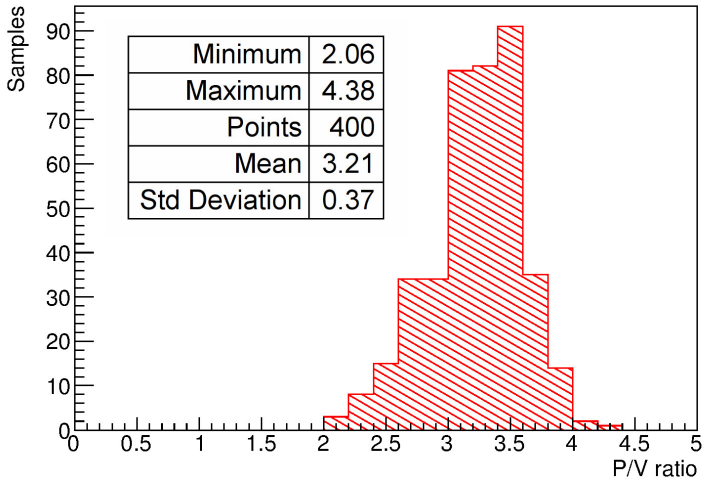

Figure 14. Distribution of the P/V ratio at room temperature for the 400 tested PMTs. Results are referred to a power supplier voltage level consistent with a gain $G = 10^7$.

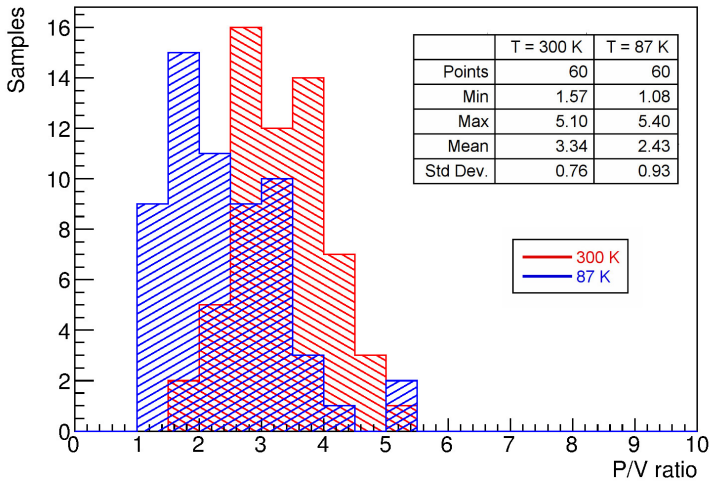

Figure 15. Comparison of the distribution of the P/V ratio at room (300 K) and at cryogenic (87 K) temperatures for 60 tested PMTs. Results are referred to a power supply consistent with a gain $G = 10^7$ at both temperatures.

The peak-to-valley P/V ratio, defined as the SER peak value divided by the minimum value to the left of the peak, is a typical indicator of the PMT capability to distinguish actual photoelectron signals from its intrinsic noise. The P/V distribution at room temperature for the 400 tested PMTs operating at $G = 10^7$ is shown in figure 14. The mean value, resulting from the SER distribution fitting, exceeds $P/V = 3 : 1$, marking very good performances of this PMT model in terms of signal/noise ratio. The variation of the P/V ratio between room and cryogenic temperature, for the 60 PMTs tested in LAr bath, is shown in figure 15. A decreases of less than 30% at cryogenic temperature, mainly due to an increase of the PMT intrinsic noise at that temperature, is observed.

2018 JINST 13 P10030

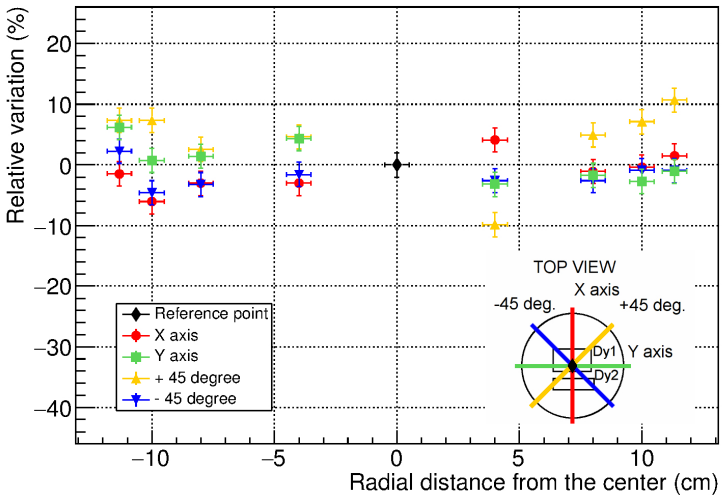

Figure 16. Variation of the photocathode response as a function of the radial distance from the window center along 4 axes oriented at 45° each other.

5.4 Photocathode uniformity

The evaluation of the photocathode uniformity required dedicated tests and was carried out for the 20 pre-series samples at room temperature, only. The PMTs were operated as photodiodes. To this purpose all the dynodes and the anode were shorted and grounded to collect all the photoelectrons emitted by the cathode which was kept at a negative voltage of about 300 V.

A collimated laser diode (Thorlabs CPS532, $\lambda = 532$ nm, 4.5 mW) was used as a continuous light source producing cathodic currents of the order of 10 µA, directly measured by a picoammeter. In order to monitor the illumination intensity and its stability, the light was split toward a photometer and the PMT which was illuminated by means of an optical fiber; a proper support was used to maintain the fiber in a fixed orientation, normal to the PMT window, while allowing to move it in various positions on the window itself.

Figure 16 shows, as example, the variation of the a photocathode response as a function of the radial distance from the window center along four different axes oriented at 45° each other. An increase of the photocathode signal approaching the window edges is recognized. This behavior was observed for all the 20 tested PMTs and it was confirmed by measurement performed by the producer.

An approximate comparison among different samples was made by averaging, for each PMT, the response data over the sensitive surface and evaluating the maximum relative variation with respect to the mean value. The resulting distribution is shown in figure 17. All the 20 PMTs show a good uniform response, within ±13% in agreement with the values indicated by the manufacturer.

5.5 Discharge and light emission

Some authors report that, at high voltage, in some PMT models it is possible to observe the presence of discharges which produce photons polluting the output signals (see for example [12]). This phenomenon is not yet well understood but it is characterized by the presence of both large light pulses (“flashes”) and microscopic processes at the SER level, also in cryogenic environment.

2018 JINST 13 P10030

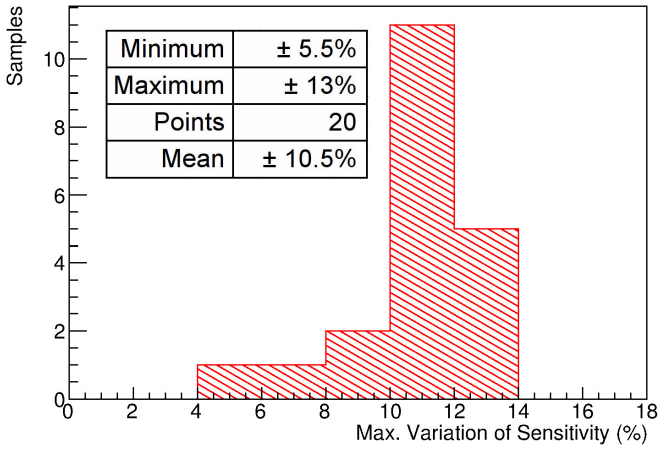

Figure 17. Distribution of the maximum variation with respect to the mean value of the PMT response for the 20 PMT samples.

A fast check of a possible presence of light emission was carried out during the characterization at cryogenic temperature of 60 PMTs. As described in section 4, measurements were performed with the simultaneous immersion of 10 PMTs in LAr. The count rate of each PMT was recorded keeping the sample under test permanently powered ON and turning, in sequence, all the other 9 specimens ON and OFF.

Variations of the count rate between the two different operating conditions were always within the statistical errors. In addition, the presence of signal coincidences beyond the expected stochastic values were excluded in the data, minimizing the possible presence of flashes or other PMT light emission phenomena that could affect the correct operation of the tested PMTs.

6 Conclusions

The updated ICARUS T600 light detection system consists of 360 Hamamatsu R5912-MOD PMTs directly operating in liquid argon to reveal scintillation photons produced by ionizing particles. A total of 400 PMTs were characterized at CERN at room temperature and 60 of them at cryogenic temperature to evaluate any parameter variation which could affect the scintillation light detection.

The main obtained results can be summarized as:

- SER and signal shape parameters are in good agreement with the producer nominal values, both at room and at cryogenic temperature;
- The resulting gain reduction at cryogenic temperature, down to 10% of the nominal value, can be on average compensated by an increase of less than 150 V of the power supply voltage;
- Dark counts and noise are in agreement with the producer nominal values at room temperature. The observed worsening at cryogenic temperature of dark counts and P/V ratio is still compatible with the correct operation of this PMT model in LAr bath;
- Good uniformity of the response of the cathode was observed all over the sensitive window;

2018 JINST 13 P10030

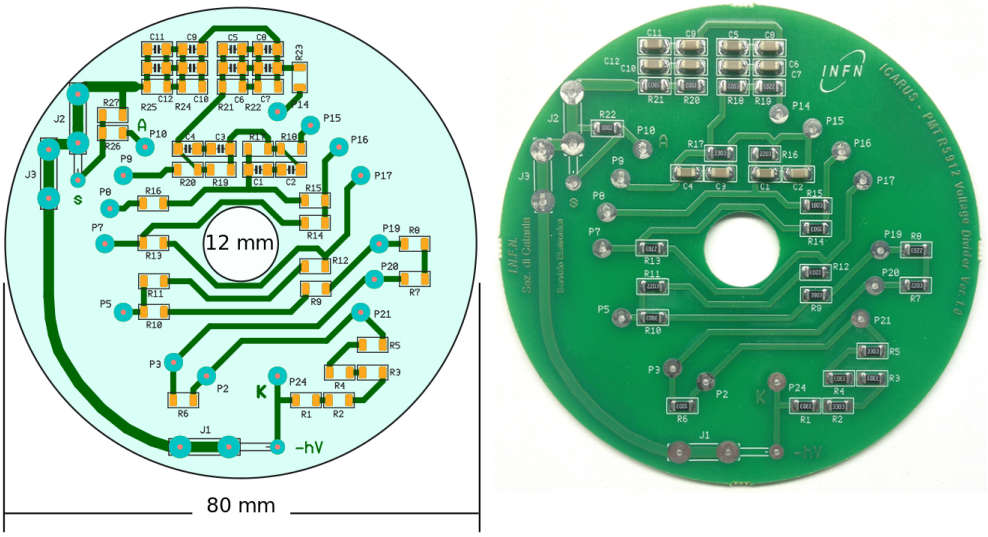

Figure 18. PMT base circuit, design (left) and picture (right).

Table 2. PMT base circuit characteristics.

Board material	FR-4
Board thickness	1.6 mm
Thrugh holes type	plated
Hole size (before plating)	0,9 mm
Copper thickness	35 µm
Soldermask	green
Silkscreen	white

- The presence of lighting phenomena were not observed;
- No mechanical damages, implosions or cracking problems were observed neither during cooling/heating phases nor operating at cryogenic temperature.

All the tested PMTs were rated as compliant with the requirements of ICARUS T600 and a subset of 360 specimens were selected for the final installation in the detector.

Acknowledgments

This work was funded by INFN in the framework of CERN WA104/NP01 program finalized to the overhauling of ICARUS detector in view of its operation on SBN at Fermilab. The staff of Hamamatsu Photonics K.K. Japan, Italy and Switzerland is acknowledged for the fruitful technical collaboration and discussion.

A Custom PMT base layout

The adopted PMT base is shown in figure 18 and the main circuit properties are presented in table 2. The resistive divider is outlined in figure 19. The reference voltage distribution ratio is the standard

2018 JINST 13 P10030

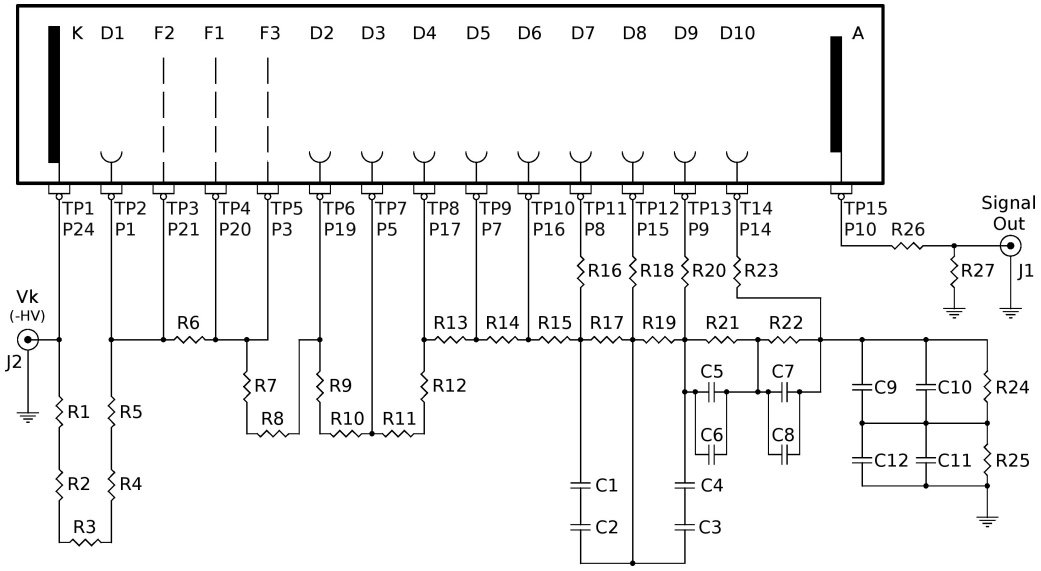

Figure 19. PMT voltage divider

Table 3. Voltage distribution ratio

Electrodes	Ratio
K-D1	16.8
D1-F2	0
F2-F1	0.6
F1-F3	0
F3-D2	3.4
D2-D3	5
D3-D4	3.33
D4-D5	1.67
D5-D6	1
D6-D7	1.2
D7-D8	1.5
D8-D9	2.2
D9-D10	3
D10-A	3.4

recommend by Hamamatsu (table 3). A particular care was devoted to the choice of damping resistors to improve the PMT time response. The 100 Ω resistors, mounted in series to each of the last three dynodes, perform a good reduction of the ringing in the output waveform.

The voltage divider chain is entirely passive, and is fabricated with SMD resistors and capacitors 1206 package (table 4), all tested in LAr bath before the mounting. The increase of the resistor value at cryogenic temperature is ≈ 3% for all the components, leaving unaffected the voltage distribution ratio of the divider. The nominal value of all the capacitors, with C0G dielectric, is maintained even at cryogenic temperature.

2018 JINST 13 P10030

Table 4. Components. All components are SMD, 1206 package, 200 V rated. Capacitors are C0G dielectric.

C1 C2 C3 C4 C5 C6 C7 C8 C9 C10 C11 C12	22 nF±5%
R1 R2 R3 R4 R5 R19	330 kΩ ± 1%
R6	100 kΩ ± 1%
R7 R8 R11 R12 R17 R21 R22	220 kΩ ± 1%
R9 R10	390 kΩ ± 1%
R13	270 kΩ ± 1%
R14 R24	150 kΩ ± 1%
R15 R25	180 kΩ ± 1%
R18 R20 R23	100 Ω ± 1%
R26	51 Ω ± 1%
R16	0 Ω

References

[1] ICARUS collaboration, S. Amerio et al., *Design, construction and tests of the ICARUS T600 detector*, *Nucl. Instrum. Meth.* **A 527** (2004) 329.

[2] C. Rubbia et al., *Underground operation of the ICARUS T600 LAr-TPC: first results*, 2011 *JINST* **6** P07011 [arXiv:1106.0975]

[3] LAr1-ND, ICARUS-WA104, MicroBooNE collaboration, M. Antonello et al., *A Proposal for a Three Detector Short-Baseline Neutrino Oscillation Program in the Fermilab Booster Neutrino Beam*, arXiv:1503.01520.

[4] A. Ankowski et al., *Characterization of ETL 9357FLA photomultiplier tubes for cryogenic temperature applications*, *Nucl. Instrum. Meth.* **A 556** (2006) 146.

[5] M. Bonesini, R. Mazza, T. Cervi, A. Menegolli, M. C. Prata, G. L. Raselli et al., *Realization of a high vacuum evaporation system for wave-length shifter deposition on photo-detector windows*, *J. Vacuum Sci. Technol.* **B 36** (2018) 01A101.

[6] M. Bonesini et al., *An innovative technique for TPB deposition on convex window photomultiplier tubes*, arXiv:1807.07123.

[7] Hamamatsu Photonics K.K., R5912-MOD data sheet (2011).

[8] A. Falcone et al., *Comparison between large area photo-multiplier tubes at cryogenic temperature for neutrino and rare event physics experiments*, *Nucl. Instrum. Meth.* **A 787** (2015) 55.

[9] P. Agnes, G.L. Raselli and M. Rossella, *Characterization of large area PMTs at cryogenic temperaturefor rare event physics experiments*, 2014 *JINST* **9** C03009.

[10] M. Babicz et al., *Timing properties of Hamamatsu R5912-MOD photomultiplier tube for the ICARUS T600 light detection system*, *Nucl. Instrum. Meth.* **A** (2018) in press.

[11] H.O. Meyer, *Dark Rate of a Photomultiplier at Cryogenic Temperatures*, arXiv:0805.0771.

[12] D.Yu. Akimov, A.I. Bolozdynya, Yu.V. Efremenko, V.A. Kaplin, A.V. Khromov, Yu.A. Melikyan et al., *Observation of light emission from Hamamatsu R11410-20 photomultiplier tubes*, *Nucl. Instrum. Meth.* **A 794** (2015) 1 [arXiv:1504.07651].

2018 JINST 13 P10030